

Constraining scalar fields with stellar kinematics and collisional dark matter

Pau Amaro-Seoane

*Max-Planck Institut für Gravitationsphysik, Albert-Einstein-Institut, Potsdam, Germany
and
Institut de Ciències de l'Espai (CSIC-IEEC), Bellaterra, Barcelona, Spain*

Juan Barranco & Argelia Bernal

Max-Planck Institut für Gravitationsphysik, Albert-Einstein-Institut, Potsdam, Germany

Luciano Rezzolla

*Max-Planck Institut für Gravitationsphysik, Albert-Einstein-Institut, Potsdam, Germany
and
Department of Physics and Astronomy Louisiana State University, Baton Rouge, LA,
USA*

ABSTRACT: The existence and detection of scalar fields could provide solutions to long-standing puzzles about the nature of dark matter, the dark compact objects at the center of most galaxies, and other phenomena. Yet, self-interacting scalar fields are very poorly constrained by astronomical observations, leading to great uncertainties in estimates of the mass m_ϕ and the self-interacting coupling constant λ of these fields. To counter this, we have systematically employed available astronomical observations to develop new constraints, considerably restricting this parameter space. In particular, by exploiting precise observations of stellar dynamics at the center of our Galaxy and assuming that these dynamics can be explained by a single boson star, we determine an upper limit for the boson star compactness and impose significant limits on the values of the properties of possible scalar fields. Requiring the scalar field particle to follow a collisional dark matter model further narrows these constraints. Most importantly, we find that if a scalar dark matter particle does exist, then it cannot account for both the dark-matter halos and the existence of dark compact objects in galactic nuclei

KEYWORDS: dark matter theory, massive black holes.

Contents

1. Introduction	1
2. Boson star generalities	3
2.1 Weak self-interaction ($\Lambda_3 \ll 1$)	4
2.2 Strong self-interaction ($\Lambda_3 \gg 1$)	5
2.3 Stability of Boson Stars	6
3. Maximum Compactness for a Boson Star	7
4. Constraining m_ϕ and λ	8
4.1 Constraints from Sgr A*	9
4.2 Constraints from NGC 4258	11
4.3 Constraints from Dark-Matter Models	12
4.4 Collecting all constraints	14
5. Conclusions	15
6. Acknowledgments	17

1. Introduction

A large number of astronomical observations little doubt about the existence of dark matter (DM) and its dominant role in the matter composition in the Universe [1]. An even larger number of candidates has been proposed to play the role of this unknown component. Among those candidates, ultra-light scalar fields have been extensively studied, providing a robust paradigm for DM particles [2, 3, 4, 5] and DE [6]. Another scalar field, the inflaton, is a crucial ingredient in inflationary cosmology [7, 8, 9]. The success of cosmological and astrophysical models that invoke scalar fields has, in addition, motivated further studies of self-gravitating systems made of scalar fields, such as non-topological solitons [10], oscillatons [11] and boson stars (BS) [12, 13].

In particular, when considering a BS the scalar field is associated with a spin-zero boson with mass m_ϕ and self-interacting coupling constant λ . The essentially unconstrained freedom in choosing the free parameters characterizing the scalar field (namely its mass and self-coupling constant), allows one to build BS- models that can account for many different astrophysical objects: from galactic dark matter halos [14, 15, 16, 17], to dark

compact objects (DCOs) like MACHOS [18, 19] and black hole candidates [20, 21, 22]. Clearly, the only way to restrict the very large space of parameters spanned by BS models is by exploiting astronomical observations and use them to set constraints on the properties of the scalar field. This is, in essence, the goal of this paper.

The recent advances in high-angular resolution instrumentation have provided the possibility to study the central regions of galaxies with unprecedented precision. Space-borne telescopes, such as the Hubble Space Telescope, and ground observations using adaptive optics have opened a new window on the innermost central regions of galactic nuclei. Particularly striking is the present ability to study the kinematics of stars or gas in regions of milliparsec scale for the Milky Way [23, 24] and of sub-parsec scale for external galaxies [25, 26, 27]. One of the most intriguing conclusions of these observations is that dark compact objects (DCOs), with masses ranging between $M_{\text{DCO}} \simeq 10^6 - 10^9 M_{\odot}$, are hosted at the center of most non-active galaxies.

In the case of our own galactic center, the study of the innermost stellar dynamics has provided very convincing evidence for the existence of a DCO associated with the radio point source Sagittarius A* (Sgr A*). The closest Keplerian orbits examined are those of the so-called ‘‘S-stars’’ (also referred to as ‘‘SO-stars’’). By following the orbit of one of them, *i.e.*, the star S2 (also referred to as SO2), the mass of Sgr A* has been estimated to be about $3.7 \times 10^6 M_{\odot}$ within a volume with radius no larger than 6.25 light-hours [24, 28]. More recent data based on 16 years of observations has reduced the uncertainty and set the mass of the central DCO to $\sim 4.1 \pm 0.6 \times 10^6 M_{\odot}$ [29, 30, 31].

Assuming that the DCO in Sgr A* is a BS, we have used the observational restrictions on the volume and mass to set substantial constraints on the mass of the scalar field and on its self-interacting coupling constant. The approach followed using the observational data for Sgr A* can be applied to any other galaxy for which there is an accurate measurement of the mass and dimensions of the central object. As a result, we have also considered the case of a nearby galaxy, NGC 4258, obtaining additional constraints, which set much tighter limits when considered in combination with those of Sgr A*.

Finally, we have considered several DM candidates and discussed how present astronomical observations can be exploited to set additional limits on the scalar-field properties invoked by these DM models [2, 14, 15, 16, 17]. While some of these constraints overlap with those obtained when considering BSs, others cover a distinct region of the space of parameters and thus imply that a scalar field that could explain the rotation curves in nearby galaxies cannot be the same composing a BS representing the DCOs in galactic nuclei.

The structure of the paper is the following one. In Sect. 2 we briefly review the properties of BSs in the two regimes of weak and strong self-interaction. Section 3 is instead dedicated to the issue of the maximum compactness of a BS, where we show that the definition of an effective maximum compactness for a BS is not only possible, but actually useful when associating BSs to DCOs in galactic centres. In Sect. 4 we therefore derive our constraints on the scalar-field properties using both considerations on BSs models and

of DM models. Finally, our conclusions are contained in Sect. 5.

2. Boson star generalities

Boson stars are solutions to the Einstein Klein-Gordon system of equations

$$G_{\mu\nu} = 8\pi G T_{\mu\nu}, \quad \left(\square - \frac{dV}{d\Phi} \right) = 0, \quad (2.1)$$

where $\square \equiv (1/\sqrt{-g})\partial_\mu[\sqrt{-g}g^{\mu\nu}\partial_\nu]$. We have adopted natural units $\hbar = c = 1$, and hence $G = 1/m_p^2$, where m_p is the Planck mass. The stress energy tensor $T_{\mu\nu}$ corresponds to a complex scalar field minimally coupled to gravity and with a scalar potential $V(|\Phi|^2)$,

$$T_{\mu\nu} = \frac{1}{2}[\partial_\mu\Phi^*\partial_\nu\Phi + \partial_\mu\Phi\partial_\nu\Phi^*] - \frac{1}{2}[\Phi^{*,\alpha}\Phi_{,\alpha} + V(|\Phi|^2)]. \quad (2.2)$$

We will restrict ourselves to the case where the potential of the scalar field is given by $V = \frac{1}{2}m_\phi^2|\Phi|^2 + \frac{\lambda}{4}|\Phi|^4$, where m_ϕ is the mass of the scalar field and λ its self-interaction coupling constant. Originally BSs were introduced by Kaup [32] and studied later by Ruffini and Bonazzola [33], who considered just the mass term in the scalar potential. The case of self-interacting scalar fields were later discussed by Colpi and collaborators in [34]. If for simplicity the scalar field is assumed to be spherically symmetric and with a harmonic time dependence, $\Phi(r, t) = \phi(r)e^{-i\omega t}$, the space-time part is static. Considering spherical symmetry, the line element can be written as $ds^2 = -B(r)dt^2 + A(r)dr^2 + r^2d\Omega^2$ and the Einstein Klein-Gordon equations reduce to a system of ordinary differential equations for the metric functions A and $\tilde{B} \equiv m_\phi^2 B/\omega^2$, and for the scalar field ϕ [34]. Additional quantities appearing in the equations are $\sigma \equiv \sqrt{4\pi/m_p^2}\phi$, which reduces to the density in the Newtonian limit, and the dimensionless self-interacting coupling constant [34]

$$\Lambda \equiv \frac{\lambda m_p^2}{4\pi m_\phi^2}. \quad (2.3)$$

The freedom of choice of λ and m_ϕ is reflected in the freedom of choosing Λ and it has been shown that even when $\lambda \ll 1$, the resulting configuration may differ significantly from the non-interacting case [34]. For sufficiently small λ , on the other hand, self-interaction may only be ignored if $\lambda \ll m_\phi^2/m_p^2$, that is, if $\Lambda \ll 1$. On the other hand, configurations with $\Lambda \gg 1$ are interesting as their masses may be comparable to those of their fermion counterparts if $\lambda \sim 1$. This illustrates the relevance of taking both regimes, $\Lambda \sim 1$ and $\Lambda \gg 1$ in the analysis of BS configurations. In the next two subsections we review them briefly for completeness and to introduce a notation that will be useful later on.

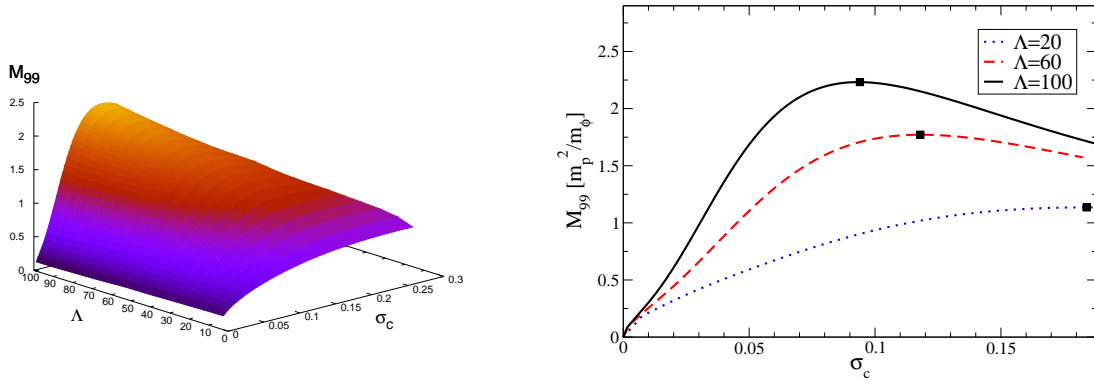


Figure 1: Gravitational mass M_{99} of equilibrium configurations of BSs for different values of σ_c and Λ in the regime $\Lambda_3 \ll 1$; black squares indicate configurations with the maximum mass. The left panel, in particular, shows a three-dimensional view of the space of solutions, while the right panel offers a view of three slices given values of Λ .

2.1 Weak self-interaction ($\Lambda_3 \ll 1$)

We next we derive equilibrium configurations for the Einstein Klein-Gordon system in the weak self-interaction regime, *i.e.*, when $\Lambda_3 \equiv \Lambda/1000 \ll 1$, following a procedure similar to the one discussed before in [12, 13, 21, 22]. In particular, in this case the Einstein Klein-Gordon system of equations can be solved as an eigenvalue problem for the radial metric function at the BS' centre \tilde{B}_c after specifying a finite but arbitrary value for the “central density” σ_c . Additional boundary conditions are those of regularity at the centre, *i.e.*, $A_c = 1$, $\sigma'_c = 0$, where the prime denotes a derivative with respect to the new dimensionless radial coordinate $x \equiv rm_\phi$, and of asymptotic flatness, *i.e.*, $\sigma(x = \infty) = 0$.

The system is solved numerically for different values of σ_c and Λ using a standard shooting method (given a σ_c , there is a unique value of \tilde{B}_c for which the boundary conditions are satisfied). Because we use a finite numerical domain, the condition for σ at infinity is in fact demanded at the outermost point of the domain x_{out} , and the shooting procedure is performed for different values of x_{out} . As x_{out} increases, the shooting parameter \tilde{B}_c converges, and we choose the solution by requiring that the condition $\sigma(x_{\text{out}}) = 0$ holds within a prescribed tolerance (*i.e.*, $\sigma(x_{\text{out}}) \lesssim 10^{-9}$).

Once the equilibrium solution is obtained, its mass is computed simply as

$$M \equiv \frac{x_{\text{out}}}{2} \left(1 - \frac{1}{A(x_{\text{out}})} \right). \quad (2.4)$$

We note that since the scalar field σ decays exponentially, the radius of the star is, at least formally, not finite. In practice, however, we define $M_{99} \equiv 0.99 M$, that is as 99% of the total gravitational mass M ; as a result, we also define R_{99} as the radius containing M_{99} and set this to be the “*effective radius*” of the BS. As a final remark we note that in view of the units adopted, both quantities M and R are dimensionless variables. The physical

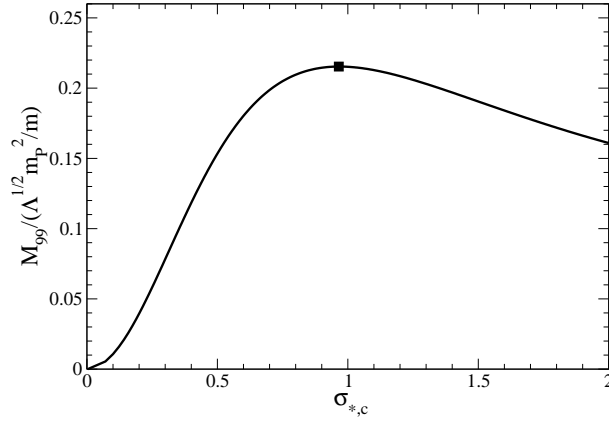


Figure 2: Gravitational mass M_{99} of equilibrium configurations of BSs for different values of σ_c in the regime $\Lambda_3 \gg 1$. Also in this case the black square indicates the configurations with the maximum mass.

units for the mass \hat{M} and radius \hat{R} can be recovered by using the following relations

$$\hat{M} = M \frac{m_P^2}{m_\phi}, \quad \hat{R} = R \frac{\hbar}{m_\phi}. \quad (2.5)$$

Figure 1 reports the gravitational mass M_{99} of equilibrium configurations of BSs for different values of σ_c and Λ in the regime $\Lambda_3 \ll 1$. In particular, the left panel shows a three-dimensional view of the space of solutions, while the right panel offers a view of three slices given values of Λ . In both panels, black squares indicate configurations with the maximum mass, thus distinguishing stable solutions (to the right of the squares) from unstable ones (see discussion in Sect. 2.3).

2.2 Strong self-interaction ($\Lambda_3 \gg 1$)

The solution of the Einstein Klein-Gordon equations is much simpler when considering instead the strong self-interaction regime, *i.e.*, when $\Lambda_3 \gg 1$. In this case, in fact, introducing the new dimensionless variables [34]

$$\sigma_* = \Lambda^{1/2} \sigma, \quad (2.6)$$

$$x_* = \Lambda^{-1/2} x. \quad (2.7)$$

and neglecting terms of order $O(\Lambda^{-1})$, the Klein-Gordon equation can be solved algebraically to yield [34]

$$\sigma_* = \left(\frac{1}{\tilde{B}} - 1 \right)^{1/2}. \quad (2.8)$$

so that $\tilde{B}_c = 1/(\sigma_{*,c}^2 + 1)$. Furthermore, the full set of the Einstein Klein-Gordon equations does not depend on Λ at first order and can be solved much more easily. As in the

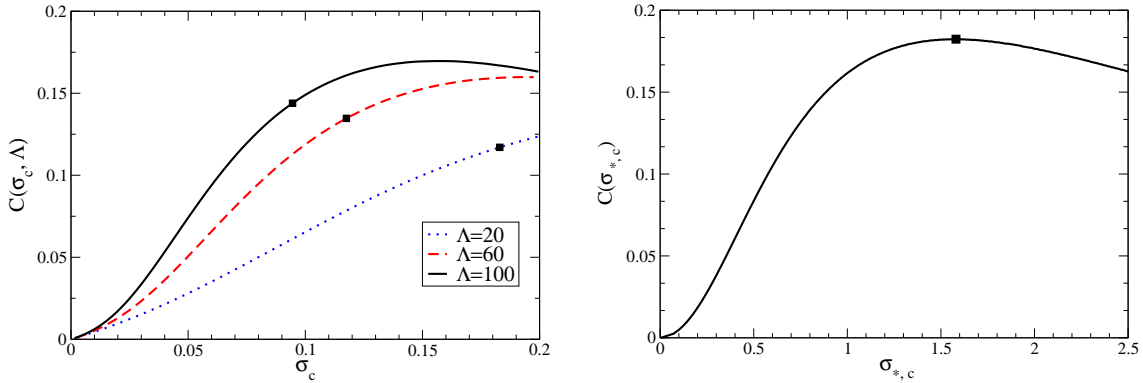


Figure 3: Effective compactness $C \equiv M_{99}/R_{99}$ for a spherical BS shown as a function of the central density σ_c . Shown in the left panel are the values in the regime of weak self-interaction $\Lambda_3 \ll 1$, while the right panel reports the values in the regime of strong self-interaction $\Lambda_3 \gg 1$. Also in this case the black squares in both panels indicates the configurations with the maximum mass.

weak self-interaction regime, equilibrium configurations are obtained solving a set of ordinary differential equations with the same boundary conditions. One important difference, however, is that in this limit the density σ does go to zero at a finite radius x_S and, as for ordinary fluid stars, the gravitational mass M is defined by Eq. (2.4) with $x_{\text{out}} = x_S$. In analogy with the previous treatment, we define the effective radius of the BS as R_{99} , namely as the one containing 99% of the total gravitational mass¹. Finally, because the introduction of the new variable x_* , see eq (2.6), the physical units can be recovered by using the following relations

$$\hat{M} = \Lambda^{1/2} M \frac{m_P^2}{m_\phi}, \quad \hat{R} = \Lambda^{1/2} R \frac{\hbar}{m_\phi}. \quad (2.9)$$

Shown in Fig. 2 is the gravitational mass M_{99} of equilibrium configurations of BSs for different values of σ_c in the regime $\Lambda_3 \gg 1$. Also in this case the black square indicates the configurations with the maximum mass, thus distinguishing stable solutions (to the right of the square) from unstable ones (see discussion in Sect. 2.3).

As a final remark, we note that a general analytic expression for the mass and compactness of a BS in the strong self-interaction regime can be given and that fits well the data presented in the right panel of Fig. 2. Such expressions are useful as they allow one to obtain simple estimates to be used in astronomical observations.

2.3 Stability of Boson Stars

Clearly, the stability of BS configurations is a basic requirement when considering them as suitable models of astrophysical objects. Numerical [35, 36] and analytical [37, 38, 39]

¹Note that since in the case $\Lambda_3 \gg 1$ the BS has a finite radius, the definition of R_{99} is strictly speaking not necessary, but it is nevertheless useful to maintain consistency with the case $\Lambda_3 \ll 1$.

stability studies of BSs agree on a general result: nodeless BS configurations are stable under finite radial perturbations if their scalar field central value σ_c is smaller than a critical value σ_{crit} ; configurations with $\sigma_c > \sigma_{\text{crit}}$, in fact, either collapse to a BH or disperse at infinity.

Note that, for any given value of Λ , the critical density σ_{crit} also marks the maximum mass corresponds the maximum mass of the BS, *i.e.*,

$$M_{\text{max}}(\Lambda) \equiv M(\sigma_c = \sigma_{\text{crit}}, \Lambda). \quad (2.10)$$

In the regime of $\Lambda_3 \ll 1$, the maximum mass clearly increases as Λ increases as shown in the two panels of Fig. 1. On the other hand, when $\Lambda_3 \gg 1$, one can exploit the fact that the system of the Einstein Klein-Gordon equations can be identified with that of a perfect-fluid star for which the effective equation of state is

$$p = \frac{4}{9}\rho_0 \left[\left(1 + \frac{3\rho}{4\rho_0} \right)^{1/2} - 1 \right]^2, \quad (2.11)$$

where

$$\rho = \frac{1}{4} \left(\frac{3}{\tilde{B}} + 1 \right) \left(\frac{1}{\tilde{B}} - 1 \right), \quad (2.12)$$

and $\rho_0 = m_\phi^4/\lambda$. Note that in the limit $\rho \ll \rho_0$ (which is equivalent to $P \ll \rho$ *i.e.*, the Newtonian limit) Eq.(2.11) reduces to $P = \rho^2/(16\rho_0)$, thus representing the equation of state of an $n = 1$ polytrope. As a result, the well-known theorems of stability of fluid stars may be applied to determine the stability of the BSs. In particular, BSs with $1/\tilde{B}_c$ smaller than a critical value $1/\tilde{B}_{\text{crit}}$ are stable, while those for which $1/\tilde{B}_c > 1/\tilde{B}_{\text{crit}}$ will either collapse to a black hole or disperse to infinity. In practice, when $\Lambda_3 \gg 1$, the maximum mass is $M_{\text{max}} \simeq 0.22$ and is attained at $\sigma_{\text{crit}} \simeq 0.97$; this is shown with a black square in Fig. 2.

3. Maximum Compactness for a Boson Star

Since we are interested in modelling astrophysical DCOs as stable BSs, it is important to determine whether or not a BS admits a maximum compactness, just as it is the case for an ordinary relativistic star. At first it may appear that this question is not even well posed as BSs are in principle infinitely extended and hence always with a zero compactness. However, even an infinitely extended BS is in practice centrally condensed, *i.e.*, with a *finite* effective radius R_{99} . Hence, it is mathematically legitimate and astrophysically reasonable to consider whether the “*effective compactness*” of a BS, defined as

$$C(\sigma_c, \Lambda) \equiv \frac{M_{99}(\sigma_c, \Lambda)}{R_{99}}, \quad (3.1)$$

and thus measuring the compactness of a BS with mass M_{99} in a radius R_{99} , can be nonzero and is even upper bounded. As we will show in what follows, this is indeed the case and $C(\sigma_c, \Lambda) \lesssim 0.16$ for all values of Λ .

Before entering the discussion of the different regimes of self-interaction it is interesting to note that if computed in terms of the physical values for the effective mass \hat{M}_{99} and effective radius \hat{R}_{99} , the compactness C is independent of m_ϕ [(cf. Eqs (2.5) and (2.9)].

In the case of weak self-interaction $\Lambda_3 \ll 1$, the compactness (3.1) is shown in the left panel of Fig. 3 for different values of Λ . Note that the compactness is a growing function of σ_c , but also that it has a local maximum. The latter, however, is reached for unstable configurations, since it refers to BSs whose central density $\sigma_c > \sigma_{\text{crit}}$. Shown in fact with black squares are the configurations with the maximum mass and these are all to the left of the local maxima: these models mark therefore the BSs with the maximum compactness for a given choice of central density and coupling constant, *i.e.*, $C_{\text{max}}(\sigma_c, \Lambda)$.

A very similar behaviour is shown by the compactness in the right panel of Fig. 3, which however refers to the regime of strong self-interaction $\Lambda_3 \gg 1$. The obvious difference in this case is that the compactness does not depend on Λ (and hence on the free parameters of the scalar field m_ϕ and λ) and attains a maximum value for stable configurations $C_{\text{max}, \Lambda_\infty} = 0.158496114$ at $\sigma_{\text{crit}} \simeq 0.97$; this is shown with a black square in the right panel Fig. 3². Interestingly, this maximum compactness is close to that of a typical neutron star with mass $M_{\text{NS}} = 1.4 M_\odot$ and a radius of $R_{\text{NS}} = 12$ km.

Comparing the two panels of Fig. 3 it is easy realize that the maximum compactness increases with Λ and has as asymptotic value for $\Lambda \rightarrow \infty$ the one given by $C_{\text{max}, \Lambda_\infty}$. This is clearly shown in Fig. 4, where we report the maximum compactness C_{max} as a function of the of coupling constant Λ . Shown with a dashed line is the asymptotic maximum compactness for a spherical BS $C_{\text{max}, \Lambda_\infty} \simeq 0.158$, while shown with a dotted and dot-dashed lines are the maximum compactnesses for a spherical star $C_{\text{max}, \text{star}} = 4/9$ [40] and the compactness of a black hole $C = 1/2$.

Overall, Fig. 4 shows two important results. The first one is that although BSs are in principle infinitely extended they can be considered to have an effective compactness which is upper limited. The second one is that such a maximum compactness is smaller than the corresponding one for a fluid star and, of course, of a black hole. To be best of our knowledge neither of these two results was discussed before in the literature.

4. Constraining m_ϕ and λ

In what follows we discuss how to make use of the astronomical observations of galactic centres (Sgr A* and NGC 4258) and of present DM models to constrain the space of possible parameters for the scalar field mass m_ϕ and self-interaction coupling constant λ . It

²Note that although $C_{\text{max}, \Lambda_\infty}$ does not consider the whole mass, the corresponding compactness 0.158496114 is very close to the maximum one obtained when considering the whole mass and the whole radius and which is given by $M_S/R_S = 0.159807753$.

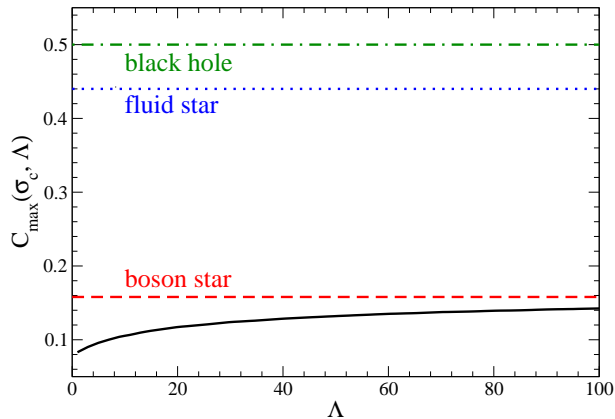


Figure 4: Maximum compactness C_{\max} shown as a function of the of coupling constant Λ . Indicated with dashed line is the asymptotic maximum compactness for a spherical BS $C_{\max, \Lambda \infty} \simeq 0.318$, while a dotted and dot-dashed lines are the maximum compactnesses for a spherical star $C_{\max, \text{star}} = 4/9$ and the compactness of a black hole $C_{\text{BH}} = 1/2$, respectively.

is however important to recall that present constraints on m_ϕ and λ are extremely loose. Previous works that considered BSs as DCOs candidates [21, 22], in fact, neither m_ϕ or λ were related to an existing particle or particle candidate. In Ref. [20], on the other hand, some first estimates were presented but not using the astronomical observations considered here.

4.1 Constraints from Sgr A*

A first set of constraints can be set by exploiting the observations about the dynamics of the S-stars around Sgr A* and in particular of the smallest measured periastron for this group of stars. This is attained for the star S2, whose periastron is $R_{\text{S2}} \simeq 17$ light-hour $\simeq 5.9 \times 10^{-4}$ pc. If a DCO is indeed hosted at the centre of Sgr A*, then its radius cannot be larger than R_{S2} or it would perturb considerably these orbits. Hence its minimum compactness is

$$C_{\min} = \frac{M_{\text{Sgr A}^*}}{R_{\text{S2}}} \simeq \frac{1}{3015}, \quad (4.1)$$

where the second equality has been obtained using the measured mass of Sgr A*, which has been estimated to be $M_{\text{Sgr A}^*} = 4.1 \pm 0.6 \times 10^6 M_\odot$ [41]³. Note that when expressed in terms of the Schwarzschild radius corresponding to Sgr A*, *i.e.*, $R_{\text{S}} = 2M_{\text{Sgr A}^*}$, the periastron of the S2 star is $R_{\text{S2}} \simeq 1520 R_{\text{S}}$.

³We note that larger compactnesses (indeed as large as the ones corresponding to a black hole) have been suggested for C_{\min} on the basis of radio observations at wavelengths of 3.5 mm and 7 mm [42, 43]. The measurements are particularly complex and may be contaminated by instrumental errors which are difficult to remove completely. In view of these uncertainties we prefer to use the more conservative but also more accurate estimate (4.1).

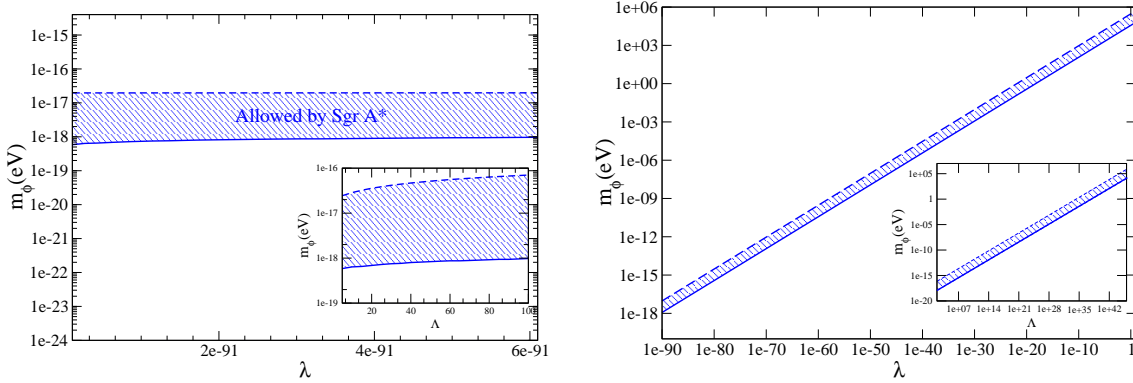


Figure 5: Constraints on the possible values of the mass and coupling constant of the complex scalar field. The left panel refers to the weak self-interaction regime of $\Lambda_3 \ll 1$, where the dashed line refers to the condition (4.3), while the solid one to the condition (4.4). The shaded region is clearly the union of the inequalities. The right panel is the same as the left one, but refers to the strong self-interaction regime of $\Lambda_3 \gg 1$, so that where the dashed line refers to (4.5), while the solid one to (4.6). In both panels shown with the insets are the same data but in terms of the dimensionless self-interacting coupling constant Λ .

The observational evidence that Sgr A* is a black hole is indeed very convincing, but we here assume, for the sake of argument, that it is rather a BS of mass $M_{\text{Sgr A}^*}$. In this case, its compactness could be in the range

$$3.32 \times 10^{-4} \simeq C_{\min} \leq C_{\text{BS}} \leq C_{\max} \simeq 0.158. \quad (4.2)$$

In other words, by changing m_ϕ and λ it is possible to construct infinite BS models that would be compatible with the observations of the S-stars and with radii between $R_{\text{S}2}$ and $R_{\min} \equiv M_{\text{Sgr A}^*}/C_{\max}$. In this way, the condition (4.2) can be used effectively to constrain the space of parameters of potential scalar fields.

The procedure adopted in practice to enforce the condition (4.2) is somewhat involved and, as in the previous Sections, we will consider separately the cases of weak and strong self-interaction. In particular, when $\Lambda_3 \ll 1$ the *maximum* value of m_ϕ compatible with the mass of Sgr A* can be set by recalling that the relation between physical and non-physical masses (2.5) states that the scalar-field mass is proportional to the BS mass for any given value of the physical mass. Hence, after fixing $M_{\text{Sgr A}^*}$, the mass of the scalar field will have to satisfy the inequality

$$m_\phi \leq \frac{M_{\max}(\Lambda)}{M_{\text{Sgr A}^*}} m_P^2. \quad (4.3)$$

The condition (4.3) when the equality holds is shown as a dashed line in the left panel of Fig. 5.

Similarly, a lower limit on m_ϕ can be found by determining, for each Λ , the central density σ_c^* and the radius $R(\sigma_c^*)$ of the BS model having the minimum compactness, C_{\min}

(we recall that the compactness is a monotonic function of C). Defining then the minimum mass as $M_{\min}(\Lambda) \equiv C_{\min} R(\sigma_c^*)$, we can constrain the mass of the scalar field to satisfy the inequality

$$m_\phi \geq \frac{M_{\min}(\Lambda)}{M_{\text{Sgr A}^*}} m_P^2. \quad (4.4)$$

The condition (4.4) when the equality holds is shown as a solid line in the left panel of Fig. 5, while the shaded region is the union of the inequalities (4.3) and (4.4).

In the regime of strong self-interaction $\Lambda_3 \gg 1$, on the other hand, we employ a technique similar to the one discussed above to obtain again upper and lower limits, with the difference that in this regime there is only a single mass curve (*cf.* Fig. 2). In this case, the maximum m_ϕ is

$$m_\phi \leq m_\phi^{\max} = \sqrt{\frac{0.22 m_P^3}{M_{\text{Sgr A}^*}}} \lambda^{1/4} \simeq 2.9 \times 10^5 \lambda^{1/4} \text{ eV}. \quad (4.5)$$

The condition (4.5) when the equality holds is shown as a dashed line in the right panel of Fig. 5. In addition, also when $\Lambda_3 \gg 1$, C_{\min} allows us to derive the lower limit of m_ϕ with the difference that the variable parameter now is just \tilde{B}_c and we do not need to iterate also on Λ . As a result we obtain

$$m_\phi \geq m_\phi^{\min} \simeq 3.7 \times 10^4 \lambda^{1/4} \text{ eV}. \quad (4.6)$$

The condition (4.4) when the equality holds is shown as a solid line in the right panel of Fig. 5, while the shaded region is the union of the inequalities (4.3) and (4.6). The overlap in the constraints between the two regimes is very good and hence the results obtained for $\Lambda_3 \gg 1$ can be easily extrapolated to the regime $\Lambda_3 \ll 1$ by using fitting expressions.

4.2 Constraints from NGC 4258

The procedure discussed above for the Galactic centre can be exploited in principle for any other galaxy for which there is an accurate measurement of the mass and dimensions of the central object. As an example, we here consider also NGC 4258, which is a spiral galaxy at a distance of about 73 – 83 Mpc. In this case, the mass of the central DCO has been estimated to be $M_{\text{NGC 4258}} = 38.1 \pm 0.01 \times 10^6 M_\odot$, while the observations of the rotation curve require a central density of at least $4 \times 10^9 M_\odot \text{ pc}^{-3}$, which implies a maximum radius $R_{\max} \simeq 36000 R_S$ [44].

Restricting our attention to the regime $\Lambda_3 \ll 1$, we show in Fig. 6 as a forward-shaded area the upper and lower limits for (m_ϕ, λ) as derived from the observations coming from NGC 4258. Similarly, in the regime $\Lambda_3 \gg 1$, the upper limit for the scalar-field mass is obtained by setting the maximum mass $m_\phi \leq m_\phi^{\max} = \sqrt{0.22 m_P^3 / M_{\text{NGC 4258}}} \lambda^{1/4}$, while the lower limit comes from the minimum compactness $C_{\min} = 1/72000$. The combined constraint can then be expressed as (not shown in Fig. 6)

$$6.3 \text{ eV} \lesssim \frac{m_\phi}{\lambda^{1/4}} \lesssim 9.6 \times 10^4 \text{ eV}. \quad (4.7)$$

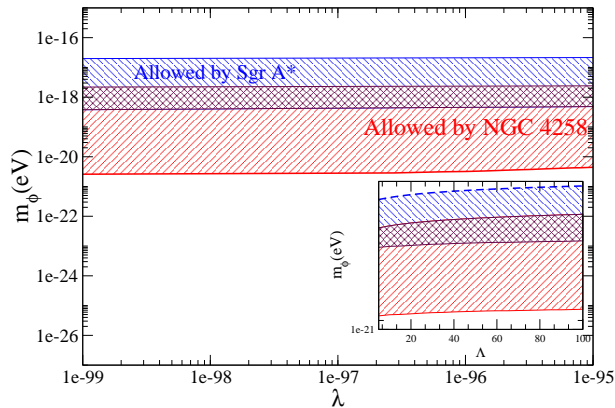


Figure 6: Constraints for m_ϕ and λ derived from the observations of NGC 4258 in the limit $\Lambda_3 \ll 1$ (forward-shaded area). Shown as a double-shaded area is the combination of the constraints coming from Sgr A* and NGC 4258. Shown with the inset is the same data but in terms of the dimensionless self-interacting coupling constant Λ .

Combining these constraints with those derived in the previous Section for Sgr A*, we obtain the following global constraints on the parameter space obtained when modelling the DCOs as BSs

$$3.7 \times 10^4 \text{ eV} \lesssim \frac{m_\phi}{\lambda^{1/4}} \lesssim 9.6 \times 10^4 \text{ eV}. \quad (4.8)$$

The corresponding region is shown as a double shaded region in Fig. 6 and clearly sets a tighter constraint on the possible values of m_ϕ and λ .

4.3 Constraints from Dark-Matter Models

As mentioned in the Introduction, constraints on the properties of the scalar field can be imposed also exploiting cosmological observations. We recall that the Lambda Cold Dark Matter model (or Λ CDM as it is usually referred to⁴) is a standard model of big bang cosmology, which attempts to explain within a single framework a number of cosmological constraints and observations. These are, for instance, the existence and properties of the cosmic microwave background, the abundances of light elements (hydrogen, helium, lithium, the large-scale structure of the universe in terms of galaxy clusters, and, more recently, also the accelerating expansion of the universe observed in the light from distant galaxies and supernovae.

In spite of its many successes, some the predictions of the Λ CDM scenario are in contrast with observations. One example is the so-called the “core/cusp problem” [45], where numerical N-body simulations assuming a Λ CDM cosmology predict the generation of diverging cusps in the central density of the DM distribution in galaxies, and which are incompatible with observations at galactic scales. Another example is the so-called

⁴Note that the Λ here is the cosmological constant and should not be confused with the self-coupling constant defined in (2.3).

the “dwarf-galaxy problem” [46], where again the Λ CDM predicts an overproduction of dwarf galaxies in the local group, which is not corroborated by observations. A possible remedy to these has come through the suggestion that DM might be treated as extremely light bosonic (dark) matter, the so-called “fuzzy dark matter” [2], or as a scalar-field (dark) matter [3, 4, 5]. Both suggestions predict flat density profiles at the center of galaxies [47] and fit the abundance of dwarf galaxies [3, 4, 5]. An alternative suggestion is that the DM particle could have a very strong self-interaction, but negligible annihilation [48]. In this case, the core/cusp problem is alleviated since the strong self-interaction increases the scattering among DM particles. The scattering cross section is then so high that collisions at the center of galaxies are very so frequent that dark matter particles scatter out the center as fast as they are accreted, thus effectively preventing a growth in the density.

In what follows we briefly summarize the main results of the scalar-field DM and the “collisional” DM scenarios and discuss how to use the present observations to further constraint the space of parameters for a complex scalar field. We recall that the collisional DM model of [48] is also referred to as “self-interacting” DM because the scattering cross section is much larger than that of standard WIMPS, that collisions among DM particles are very frequent. On the other hand, the prototype of a DM candidate consisting of ultra-light scalar field is the axion, which has been introduced as a solution to the strong CP problem [49, 50]. The mass of the axion has been estimated to be in the range $10^{-5} \text{ eV} \lesssim m_a \lesssim 10^{-3} \text{ eV}$ [51]. However, in order to explain the singular galactic core and suppress the formation of dwarf galaxies, the axion’s mass should be orders of magnitude smaller. In the absence of self-interaction, the mass should in fact be $m_\phi \sim 10^{-22} - 10^{-24} \text{ eV}$, which then gives a reasonable fit to the rotation curves [14, 15].

At the same time, the cosmological study of the scalar-field DM performed in [3, 52, 53] for different potentials $V(\phi)$ have shown to be able to reproduce all the features of the standard Λ CDM in the linear regime of perturbations. Furthermore, a DM model with a complex scalar field having a quartic potential was studied in [17], and the fit of rotational curves for dwarf galaxies was shown to be robust provided that

$$2.7 \text{ eV} \lesssim \frac{m_\phi}{\lambda^{1/4}} \lesssim 2.9 \text{ eV}. \quad (4.9)$$

This is shown as a thick solid line in Fig. 7.

A different suggestion has been made in Ref. [48], where the DM is proposed to be cold, non-dissipative and self-interacting with a scattering cross-section per particle mass given by

$$\frac{\sigma_{2 \rightarrow 2}}{m_\phi} = 10^{-25} - 10^{-23} \frac{\text{cm}^2}{\text{GeV}}, \quad (4.10)$$

and independent of the particle itself. This model solves the small scale problems of Λ CDM and N -body numerical simulation confirms this [54]. Since the conjecture is made without assuming a particular model for DM, we can derive the values for (m_ϕ, λ) for a scalar field with self-interaction. For that, we introduce as the interacting potential

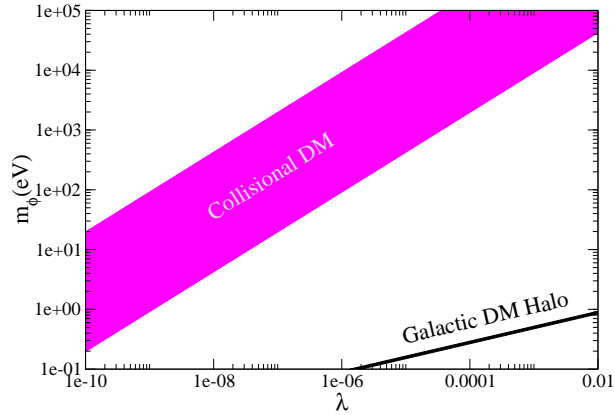


Figure 7: The constraints on m_ϕ and λ coming from the different DM models. Shown with a dashed magenta area the allowed values for coming from the collisional DM model, while shown with a black region are the corresponding values as constrained from the measurement of the DM halo.

$V = \lambda\phi^4/4$. Thus, the scattering matrix element is $\mathcal{M}(\phi\phi \rightarrow \phi\phi) = i\lambda$ and the resulting cross-section is

$$\sigma(\phi\phi \rightarrow \phi\phi) = \sigma_{\phi\phi} = \frac{\lambda^2}{16\pi s} = \frac{\lambda^2}{64\pi m_\phi^2}, \quad (4.11)$$

since the square of the center of mass energy is $s = 4m_\phi^2$. By requiring that the cross-section of Eq. (4.11) has the strength of the collisional DM of Eq. (4.10), we find that m_ϕ must be

$$9.5 \times 10^5 \text{ eV} \lesssim \frac{m_\phi}{\lambda^{2/3}} \lesssim 9.5 \times 10^7 \text{ eV}. \quad (4.12)$$

The constraints coming from the different DM models are summarized in Fig. 7, where we show with a dashed magenta area the allowed values for m_ϕ and λ coming from the collisional DM model [cf. eq. (4.10)], while shown with a black region are the corresponding values as constrained from the measurement of the DM halo [cf. eq. (4.9)].

4.4 Collecting all constraints

We can combine all of the constraints derived so far and conclude that a scalar field which can account for DM candidate and fulfill the constraints imposed by the observations on the DCO at the center of our Galaxy and NGC 4258 must have a mass and a self-interacting coupling constant in the ranges

$$\begin{aligned} 6.5 \times 10^{-9} &\lesssim \lambda \lesssim 4.2 \times 10^{-3}, \\ 332 \text{ eV} &\lesssim m_\phi \lesssim 2.46 \times 10^4 \text{ eV}. \end{aligned} \quad (4.13)$$

This region is marked as “combined” in Fig. 8, which reports also the constraints coming from modelling the DCOs as BSs and discussed in the previous Sections.

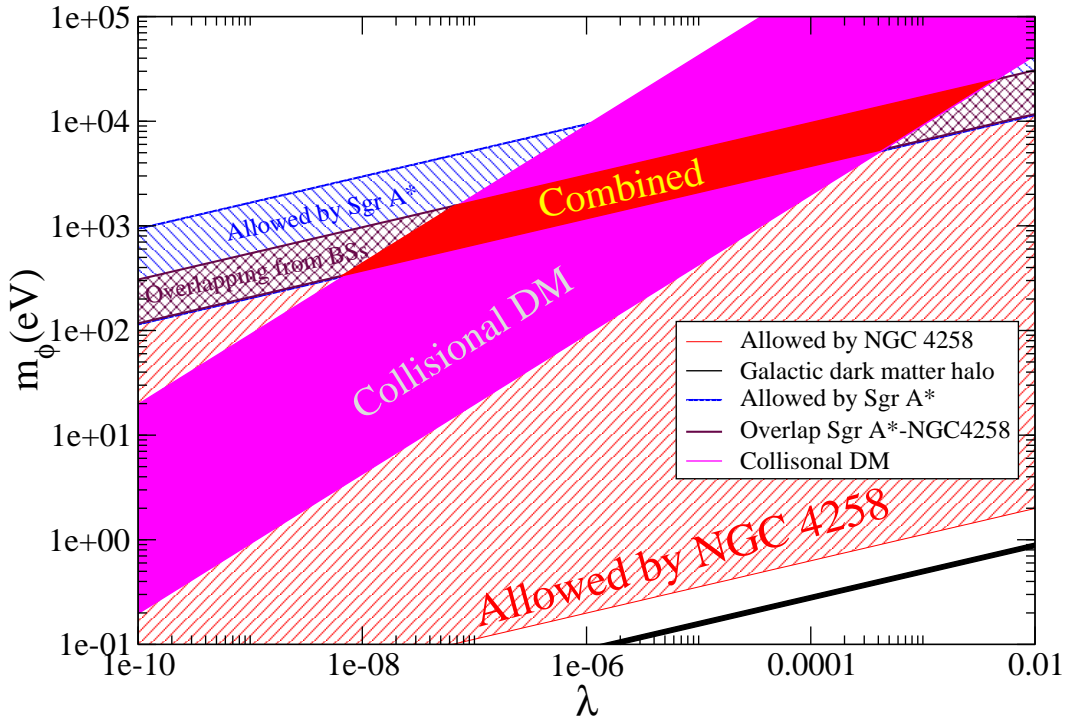


Figure 8: Constraints on (m_ϕ, λ) based on available stellar kinematic data for Sgr A* (narrow upper stripe filled with solid blue lines), as well as for NGC 4258 (broad lower stripe filled with dashed orange lines) and their intersection (middle stripe filled with black crosses). The solid magenta stripe that crosses all other stripes is derived from the requirement of collisional DM and demarcates the combined restrictions (red solid region). We also show the limits on the parameters derived from the models of galactic DM halos based on scalar fields (solid black line).

We also note that although the lower limit of the region constrained from the observations of NGC 4258 is not too far from the limit set by condition (4.9), the latter is at least four orders of magnitude smaller than the region representing the overlap between collisional DM models and the kinematic constraints from galactic observations. As a result, we conclude that a scalar field that could explain the rotation curves in nearby galaxies cannot be the same composing a BS representing the DCOs in galactic nuclei.

5. Conclusions

We have used the most accurate astronomical observations on the kinematics of galaxy centres to set constraints on the mass m_ϕ and self-interaction constant λ of complex scalar fields, which have been employed in the literature to model BSs as DCOs in galactic centres or as DM candidates on cosmological scales. More specifically, we have used the estimates of the mass and volume for the nucleus of our Galaxy and of NGC

4258 to limit the possible models of BSs when these are advocated to account for such observations.

These constraints, together with those obtained by considering possible DM candidates have allowed us to restrict the possible values of m_ϕ and λ to the ranges

$$6.5 \times 10^{-9} \lesssim \lambda \lesssim 4.2 \times 10^{-3},$$

$$332 \text{ eV} \lesssim m_\phi \lesssim 2.46 \times 10^4 \text{ eV},$$

that is to a region that spans six orders of magnitude for λ and one order of magnitude for m_ϕ . To the best of our knowledge, these constraints for the scalar field are by far tighter than any other discussed so far in astrophysical or cosmological context. In addition, since the space of parameters has two non-overlapping constrained regions, we conclude that a scalar field that could explain the rotation curves in nearby galaxies cannot be the same composing a BS representing the DCOs in galactic nuclei.

Our analysis here has been limited to the simplest possible scenario in which the DCO is not a black hole but a BS. A much more realistic configuration, however, is one in which the BS hosts at its centre a massive black hole of comparable mass, *i.e.*, a *hybrid-BS*. Mixed models for BS have been proposed in the past, for instance when studying the boundary between stable and unstable equilibrium configurations of cold boson-fermion stars (see [55, 12] and references therein).

A mixed model with a BH in the center is more realistic because for a number of reasons. First, as long as the size of the black-hole horizon is much smaller than the scalar-field Compton length, the accretion of the scalar field onto the black hole is very small [56] and hence a stationary model can be constructed (if this was not the case the scalar field would eventually be all accreted by the black hole). Second, they automatically satisfy all the constraints usually set when considering the DCO as a massive black hole. Finally, by having a black hole at its centre, a hybrid BS does not need to account for the electromagnetic emission that would be otherwise produced by the matter condensing and heating-up at the centre of an ordinary BS.

Together with these advantages, however, a hybrid-BS model has the important drawback that it may be very difficult to distinguish it from a pure black-hole solution, the differences being so small that they may be below the present (and possibly future) observational limits from electromagnetic radiation. In this respect, the gravitational-wave observations that will be made possible by the space-borne LISA mission, may well be determinant. LISA will in fact detect a large number of extreme-mass ratio inspirals or EMRIs (see, [57] for a recent review) and because the associated gravitational waveforms probe a region of the spacetime very close to the black hole, they may work as telltale about the presence of a scalar field surrounding the black hole. Some work on the effects of matter fields on the gravitational-wave emission from EMRIs has already been done [58, 59], and extending this question also to scalar fields will be the focus of our future research.

6. Acknowledgments

It is a pleasure to thank Marc Freitag for useful discussions and Rainer Schödel for input on the observational aspects. We are grateful to Philippe Jetzer, and David J. Vanecek for their comments on the manuscript. This work was supported in part by the DFG grant SFB/Transregio 7 “Gravitational-Wave Astronomy”.

References

- [1] G. Bertone, D. Hooper, and J. Silk, *Particle dark matter: evidence, candidates and constraints*, *Phys. Rept.* **405** (2005) 279–390
- [2] W. Hu, R. Barkana, and A. Gruzinov, *Fuzzy Cold Dark Matter: The Wave Properties of Ultralight Particles*, *Phys. Rev. Lett.* **85** (2000) 1158–1161
- [3] T. Matos and L. A. Ureña-López, *Quintessence and scalar dark matter in the Universe*, *Class. and Quant. Grav.* **17** (2000) L75–L81
- [4] T. Matos and L. Arturo Ureña-López, *Further analysis of a cosmological model with quintessence and scalar dark matter*, *Phys. Rev. D* **63** (2001) 063506
- [5] T. Matos and L. A. Ureña-López, *On the Nature of Dark Matter*, *Int. J. Mod. Phys. D* **13** (2004) 2287–2291
- [6] J. A. Frieman, C. T. Hill, A. Stebbins, and I. Waga, *Cosmology with Ultralight Pseudo Nambu-Goldstone Bosons*, *Phys. Rev. Lett.* **75** (1995) 2077–2080
- [7] A. H. Guth, *Inflationary universe: A possible solution to the horizon and flatness problems*, *Phys. Rev. D* **23** (1981) 347–356.
- [8] A. D. Linde, *A new inflationary universe scenario: A possible solution of the horizon, flatness, homogeneity, isotropy and primordial monopole problems*, *Phys. Lett. B* **108** (1982) 389–393.
- [9] A. Albrecht, P. J. Steinhardt, M. S. Turner, and F. Wilczek, *Reheating an inflationary universe*, *Phys. Rev. Lett.* **48** (1982) 1437–1440.
- [10] T. D. Lee, *Soliton stars and the critical masses of black holes*, *Phys. Rev. D* **35** (1987) 3637–3639.
- [11] L. A. Ureña-López, *Oscillatons revisited*, *Class. and Quant. Grav.* **19** (2002) 2617–2632
- [12] P. Jetzer, *Boson stars*, *Phys. Rept.* **220** (1992) 163–227.
- [13] F. E. Schunck and E. W. Mielke, *TOPICAL REVIEW: General relativistic boson stars*, *Class. and Quant. Grav.* **20** (2003) 301.
- [14] A. Arbey, J. Lesgourgues, and P. Salati, *Quintessential halos around galaxies*, *Phys. Rev. D* **64** (2001) 123528

- [15] A. Arbey, J. Lesgourgues, and P. Salati, *Cosmological constraints on quintessential halos*, *Phys. Rev. D* **65** (2002) 083514
- [16] T. Matos and L. A. Ureña-López, *Flat rotation curves in scalar field galaxy halos*, *Gen. Rel. Grav.* **39** (2007) 1279–1286.
- [17] A. Arbey, J. Lesgourgues, and P. Salati, *Galactic halos of fluid dark matter*, *Phys. Rev. D* **68** (2003) 023511
- [18] X. Hernández, T. Matos, R. A. Sussman, and Y. Verbin, *Scalar field “mini-MACHOs”: A new explanation for galactic dark matter*, *Phys. Rev. D* **70** (2004) 043537
- [19] J. Barranco and A. Bernal, *Self-gravitating system made of axions*, *ArXiv e-prints* (2010) [arXiv:1001.1769].
- [20] D. F. Torres, S. Capozziello, and G. Lambiase, *Supermassive boson star at the galactic center?*, *Phys. Rev. D* **62** (2000) 104012
- [21] F. S. Guzmán, *Accretion disk onto boson stars: A way to supplant black hole candidates*, *Phys. Rev. D* **73** (2006) 021501
- [22] F. S. Guzmán and J. M. Rueda-Becerril, *Spherical boson stars as black hole mimickers*, *Phys. Rev. D* **80** (2009) 084023.
- [23] A. M. Ghez, S. Salim, S. D. Hornstein, A. Tanner, J. R. Lu, M. Morris, E. E. Becklin, and G. Duchêne, *Stellar Orbits around the Galactic Center Black Hole*, *Astrophys. J.* **620** (2005) 744–757.
- [24] R. Schödel, T. Ott, R. Genzel, A. Eckart, N. Mouawad, and T. Alexander, *Stellar Dynamics in the Central Arcsecond of Our Galaxy*, *Astrophys. J.* **596** (2003) 1015–1034.
- [25] L. Ferrarese and H. Ford, *Supermassive Black Holes in Galactic Nuclei: Past, Present and Future Research*, *Space Science Reviews* **116** (2005) 523–624.
- [26] J. M. Moran, L. J. Greenhill, and J. R. Herrnstein, *Observational Evidence for Massive Black Holes in the Centers of Active Galaxies*, *Journal of Astrophysics and Astronomy* **20** (1999) 165.
- [27] J. Kormendy, *The Stellar-Dynamical Search for Supermassive Black Holes in Galactic Nuclei*, in “*Coevolution of Black Holes and Galaxies*”, *Carnegie Observatories, Pasadena* (L. Ho, ed.), 2003.
- [28] A. M. Ghez, G. Duchêne, K. Matthews, S. D. Hornstein, A. Tanner, J. Larkin, M. Morris, E. E. Becklin, S. Salim, T. Kremenek, D. Thompson, B. T. Soifer, G. Neugebauer, and I. McLean, *The First Measurement of Spectral Lines in a Short-Period Star Bound to the Galaxy’s Central Black Hole: A Paradox of Youth*, *Astrophys. J. Lett.* **586** (2003) L127–L131.

- [29] F. Eisenhauer, R. Genzel, T. Alexander, R. Abuter, T. Paumard, T. Ott, A. Gilbert, S. Gillessen, M. Horrobin, S. Trippe, H. Bonnet, C. Dumas, N. Hubin, A. Kaufer, M. Kissler-Patig, G. Monnet, S. Ströbele, T. Szeifert, A. Eckart, R. Schödel, and S. Zucker, *SINFONI in the Galactic Center: Young Stars and Infrared Flares in the Central Light-Month*, *Astrophys. J.* **628** (2005) 246–259.
- [30] A. M. Ghez, S. Salim, N. N. Weinberg, J. R. Lu, T. Do, J. K. Dunn, K. Matthews, M. R. Morris, S. Yelda, E. E. Becklin, T. Kremenek, M. Milosavljevic, and J. Naiman, *Measuring Distance and Properties of the Milky Way’s Central Supermassive Black Hole with Stellar Orbits*, *Astrophys. J.* **689** (2008) 1044–1062.
- [31] S. Gillessen, F. Eisenhauer, S. Trippe, T. Alexander, R. Genzel, F. Martins, and T. Ott, *Monitoring Stellar Orbits Around the Massive Black Hole in the Galactic Center*, *Astrophys. J.* **692** (2009) 1075–1109.
- [32] D. J. Kaup, *Klein-Gordon Geon*, *Phys. Rev.* **172** (1968) 1331–1342.
- [33] R. Ruffini and S. Bonazzola, *Systems of Self-Gravitating Particles in General Relativity and the Concept of an Equation of State*, *Phys. Rev.* **187** (1969) 1767–1783.
- [34] M. Colpi, S. L. Shapiro, and I. Wasserman, *Boson stars - Gravitational equilibria of self-interacting scalar fields*, *Phys. Rev. Lett.* **57** (1986) 2485–2488.
- [35] E. Seidel and W. Suen, *Dynamical evolution of boson stars: Perturbing the ground state*, *Phys. Rev. D* **42** (1990) 384–403.
- [36] S. H. Hawley and M. W. Choptuik, *Boson stars driven to the brink of black hole formation*, *Phys. Rev. D* **62** (2000) 104024.
- [37] M. Gleiser and R. Watkins, *Gravitational stability of scalar matter*, *Nucl. Phys. B* **319** (1989) 733–746.
- [38] T. D. Lee and Y. Pang, *Stability of mini-boson stars*, *Nucl. Phys. B* **315** (1989) 477–516.
- [39] F. V. Kusmartsev, E. W. Mielke, and F. E. Schunck, *Gravitational stability of boson stars*, *Phys. Rev. D* **43** (1991) 3895–3901.
- [40] H. A. Buchdahl, *General Relativistic Fluid Spheres*, *Phys. Rev.* **116** (1959) 1027–1034.
- [41] R. Genzel, F. Eisenhauer, and S. Gillessen, *The Massive Black Hole and Nuclear Star Cluster in the Center of the Milky Way*, *ArXiv e-prints* (2010) [arXiv:1006.0064].
- [42] S. S. Doeleman, J. Weintroub, A. E. E. Rogers, R. Plambeck, R. Freund, R. P. J. Tilanus, P. Friberg, L. M. Ziurys, J. M. Moran, B. Corey, K. H. Young, D. L. Smythe, M. Titus, D. P. Marrone, R. J. Cappallo, D. Bock, G. C. Bower, R. Chamberlin, G. R. Davis, T. P. Krichbaum, J. Lamb, H. Maness, A. E. Niell, A. Roy, P. Strittmatter, D. Werthimer, A. R. Whitney, and D. Woody, *Event-horizon-scale structure in the supermassive black hole candidate at the Galactic Centre*, *Nature* **455** (2008) 78–80.

- [43] S. Doeleman, E. Agol, D. Backer, F. Baganoff, G. C. Bower, A. Broderick, A. Fabian, V. Fish, C. Gammie, P. Ho, M. Honman, T. Krichbaum, A. Loeb, D. Marrone, M. Reid, A. Rogers, I. Shapiro, P. Strittmatter, R. Tilanus, J. Weintraub, A. Whitney, M. Wright, and L. Ziurys, *Imaging an Event Horizon: submm-VLBI of a Super Massive Black Hole*, in *astro2010: The Astronomy and Astrophysics Decadal Survey*, vol. 2010 of *ArXiv Astrophysics e-prints*, pp. 68, 2009. [arXiv:0906.3899](https://arxiv.org/abs/0906.3899).
- [44] J. R. Herrnstein, J. M. Moran, L. J. Greenhill, and A. S. Trotter, *The Geometry of and Mass Accretion Rate through the Maser Accretion Disk in NGC 4258*, *Astrophys. J.* **629** (2005) 719–738.
- [45] J. F. Navarro, C. S. Frenk, and S. D. M. White, *A Universal Density Profile from Hierarchical Clustering*, *Astrophys. J.* **490** (1997) 493.
- [46] A. Klypin, A. V. Kravtsov, O. Valenzuela, and F. Prada, *Where Are the Missing Galactic Satellites?*, *Astrophys. J.* **522** (1999) 82–92.
- [47] A. Bernal, T. Matos, and D. Núñez, *Flat Central Density Profiles from Scalar Field Dark Matter Halos*, *Revista Mexicana de Astronomía y Astrofísica* **44** (2008) 149–160.
- [48] D. N. Spergel and P. J. Steinhardt, *Observational Evidence for Self-Interacting Cold Dark Matter*, *Phys. Rev. Lett.* **84** (2000) 3760–3763.
- [49] R. D. Peccei and H. R. Quinn, *CP conservation in the presence of pseudoparticles*, *Phys. Rev. Lett.* **38** (1977) 1440–1443.
- [50] R. D. Peccei and H. R. Quinn, *Constraints imposed by CP conservation in the presence of pseudoparticles*, *Phys. Rev. D* **16** (1977) 1791–1797.
- [51] G. G. Raffelt, *Astrophysical Axion Bounds*, in *Axions* (M. Kuster, G. Raffelt, & B. Beltrán, ed.), vol. 741 of *Lecture Notes in Physics*, Berlin Springer Verlag, pp. 51, 2008.
- [52] T. Matos, J. Luévano, I. Quiros, L. A. Ureña-López, and J. A. Vázquez, *Dynamics of scalar field dark matter with a cosh-like potential*, *Phys. Rev. D* **80** (2009) 123521.
- [53] T. Matos, A. Vázquez-González, and J. Magaña, *Phi square as dark matter*, *Monthly Notices of the Royal Astronomical Society* **393** (2009) 1359–1369.
- [54] R. Davé, D. N. Spergel, P. J. Steinhardt, and B. D. Wandelt, *Halo Properties in Cosmological Simulations of Self-interacting Cold Dark Matter*, *Astrophys. J.* **547** (2001) 574–589.
- [55] P. Jetzer, *Stability of combined boson-fermion stars*, *Phys. Lett. B* **243** (1990) 36–40.
- [56] L. A. Ureña-López and A. R. Liddle, *Supermassive black holes in scalar field galaxy halos*, *Phys. Rev. D* **66** (2002) 083005.
- [57] P. Amaro-Seoane, J. R. Gair, M. Freitag, M. C. Miller, I. Mandel, C. J. Cutler, and S. Babak, *Intermediate and extreme mass-ratio inspirals. Astrophysics, science applications and detection using LISA*, *Class. and Quant. Grav.* **24** (2007) 113.

- [58] E. Barausse, L. Rezzolla, D. Petroff, and M. Ansorg, *Gravitational waves from extreme mass ratio inspirals in nonpure Kerr spacetimes*, *Phys. Rev. D* **75** (2007) 064026.
- [59] E. Barausse and L. Rezzolla, *Influence of the hydrodynamic drag from an accretion torus on extreme mass-ratio inspirals*, *Phys. Rev. D* **77** (2008) 104027.